



Università degli Studi Mediterranea di Reggio Calabria
Archivio Istituzionale dei prodotti della ricerca

Using random forest and multiple-regression models to predict changes in surface runoff and soil erosion after prescribed fire

This is the peer reviewed version of the following article:

Original

Using random forest and multiple-regression models to predict changes in surface runoff and soil erosion after prescribed fire / Zema, Da; Parhizkar, M; Plaza-Alvarez, Pa; Xu, Xz; Lucas-Borja, Me. - In: MODELING EARTH SYSTEMS AND ENVIRONMENT. - ISSN 2363-6203. - 0:0(2024), pp. 1-19. [10.1007/s40808-023-01838-8]

Availability:

This version is available at: <https://hdl.handle.net/20.500.12318/141562> since: 2024-11-22T11:11:06Z

Published

DOI: <http://doi.org/10.1007/s40808-023-01838-8>

The final published version is available online at: <https://link.springer.com/article/10.1007/s40808-023-01838-8>

Terms of use:

The terms and conditions for the reuse of this version of the manuscript are specified in the publishing policy. For all terms of use and more information see the publisher's website

Publisher copyright

This item was downloaded from IRIS Università Mediterranea di Reggio Calabria (<https://iris.unirc.it/>) When citing, please refer to the published version.

(Article begins on next page)

14 January 2025

1 *This is the peer reviewed version of the following article:*
2

3 **Zema, D.A., Parhizkar, M., Plaza-Alvarez, P.A., Xu, X., Lucas-Borja, M.E. 2024. *Using***
4 ***random forest and multiple-regression models to predict changes in surface runoff and soil***
5 ***erosion after prescribed fire. Modeling Earth Systems and Environment (Springer),***

6
7 *which has been published in final doi*

8
9 10.1007/s40808-023-01838-8

10
11 (<https://link.springer.com/article/10.1007/s40808-023-01838-8>)

12
13 *The terms and conditions for the reuse of this version of the manuscript are specified in the*
14 *publishing policy. For all terms of use and more information see the publisher's website*

15 **Using Random Forest and Multiple-regression models to predict changes in surface runoff and soil erosion**
16 **after prescribed fire**

17
18 **Abstract**

19
20 Prescribed fire is a viable practice to reduce the wildfire risk in forests, but its application may lead to increased
21 surface runoff and soil erosion. Several hydrological and erosive models have been proposed and evaluated to
22 predict the changes in soil hydrology and erosion after prescribed fire. However, the prediction capacity of machine
23 learning and Multiple-Regression models has scarcely been studied in sites treated with prescribed fire, despite of
24 the usefulness of these tools for landscape planners. This study aims to evaluate how a Random Forest, RF,
25 algorithm and Multiple-Regression, MR, and Partial Least Square Regression, PLS-R, equations can predict changes
26 in surface runoff and soil erosion after prescribed fire. This prediction capacity has been quantified through the
27 application of the models to 35 case studies reported in 18 academic papers selected from the international scientific
28 literature. The model predictions have been evaluated using common statistics and indexes (e.g., the coefficient of
29 Nash and Sutcliffe, NSE). The results show poor performance of the RF and PLS-R models in predicting runoff
30 ($NSE < 0$ and < 0.31). However, the models' capacity to predict soil erosion was acceptable ($NSE = 0.47$ and 0.69 ,
31 respectively). The predictions by the MR equation were also acceptable for runoff ($NSE < 0.69$) and good for
32 erosion ($NSE = 0.80$). Furthermore, the MR equation offers a large applicability, since this simple model has been
33 tested using a database of hydrological observations in environments with different characteristics. The performance
34 of MR equations is encouraging when its broader use in runoff and erosion predictions in soils treated with
35 prescribed fire.

36
37 **Keywords** Soil hydrology; wildfire risk; machine learning; regression analysis; hydrological modelling.

38
39 **Introduction**

40
41 Prescribed fire is an effective tool to reduce wildfire risk in rural areas (forests, pastures and croplands) and, as such,
42 has been applied in several countries (Klimas et al. 2020). Prescribed fire treatments generally have a low severity
43 and intensity, and the soil temperature is much lower compared to wildfires (Cawson et al. 2016). However,
44 prescribed fire removes almost all litter cover and understory vegetation, leaving the soil exposed to rainfall
45 erosivity (Hueso-González et al. 2018). Furthermore, the changes in some soil properties may be noticeable (e.g.,
46 reduction in organic matter content and thus hydraulic conductivity (Alcañiz et al. 2018)), and soil water repellency
47 may occur or noticeably increase after a prescribed fire (Pierson et al. 2008; Cawson et al. 2016).

48 These impacts of prescribed fire on soil generally result in noticeable changes in runoff and erosion rates as well as
49 alterations in the water quality of streams for some months after its application (Carrà et al. 2022; Beyene et al.
50 2023). For instance, Cawson et al. (2012) and Shakesby et al. (2015) report increases in runoff and erosion of one to
51 two orders of magnitude when compared to unburned areas. These increases occur especially in the so-called
52 'window of disturbance', a period lasting some months from prescribed fire's application (Prosser and Williams
53 1998). In contrast, according to Coelho et al. (2004), and de Dios Benavides-Solorio and MacDonald (2005),
54 prescribed fire generally results in minimal erosion. Furthermore, Keesstra et al. (2014) found lower erosion rates in

55 sites burned with prescribed fire as compared to unburned forests. These contrasting results are mainly due to
56 complex, highly dynamic and constantly changing hydrological processes in burned sites (Cao et al. 2022).
57 When they occur, the changes in soil hydrology after prescribed fire can induce severe flooding, erosion and
58 landslides. To control and mitigate the associated risks, accurate predictions of post-fire runoff and erosion in sites
59 treated with prescribed fire are essential (Morris et al. 2014). Computer-based models are generally able to predict
60 the changes in hydrological and erosive variables resulting from complex natural processes and land management
61 actions. These models may be of a different nature (e.g., empirical, physically-based and conceptual) and show
62 different complexity and variable requirements of the input data (Merritt et al. 2003; Aksoy and Kavvas 2005).
63 Therefore, choosing the most suitable model for a specific environment is difficult, and landscape managers and
64 hydrologists need practical guidance to make this choice. Their planning and management tasks are complex, due to
65 the large variability of environmental conditions.

66 Runoff and erosion in burned sites have been modelled using many prediction models in several environments (e.g.,
67 Rulli et al. 2013; Fernández and Vega 2016; Salis et al. 2019). Hydrological applications have tested empirical (e.g.,
68 SCS-CN and USLE-family models, Larsen and MacDonald 2007; Soulis 2018), semi-empirical (e.g., MMF,
69 Hosseini et al. 2018; Vieira et al. 2018b), and more complex models (e.g., PESERA and WEPP models,
70 Karamesouti et al. 2016; Fernández and Vega 2018) to predict the hydrological and erosive response of forest soils
71 affected by wildfires. Studies showing modelling applications in sites treated with prescribed fire are much fewer
72 (e.g., Lucas-Borja et al. 2020; Zema et al. 2022). To summarize, Lucas-Borja et al. (2020) applied linear regression
73 equations and the SCS-CN model to predict surface runoff in the pine forests of Central-Eastern Spain. In three
74 forest stands in Southern Italy, Carrà et al. (2021) found accurate predictions of runoff and soil loss using the SCS-
75 CN and USLE-M models, while the simulations by Horton and MUSLE equations were poor. Despite the
76 encouraging results from when using these models, these studies are limited in number, to common empirical
77 models and also confined to specific environments. In contrast, at least to the authors' best knowledge, no
78 evaluations of more complex models, such as machine learning algorithms or Multiple-Regression techniques, are
79 available in areas treated with prescribed fire. Compared to the empirical models, these prediction tools may better
80 capture the complexity of post-fire soil hydrology and offer larger applicability in environments with different
81 climatic, soil and vegetation characteristics.

82 To fill this gap, this study aims to evaluate whether changes in surface runoff and soil erosion after prescribed fire
83 can be predicted worldwide using Random Forest (a machine learning algorithm), and Multiple-Regression and
84 Partial Least Square Regression models (two multivariate statistical models). To this aim, these three models have
85 been applied to a dataset of 35 case studies found in the international scientific literature.

86

87 **Materials and Methods**

88

89 *Paper selection*

90

91 Comprehensive bibliographic research was carried out in late January 2023 on Scopus[®], Web of Science[®] and
92 Google[®] Scholar[®] databases, to find academic papers, relevant to prescribed fire and soil hydrology, published
93 between the year 2000 and the present. The following individual keywords or combination of keywords were used:

94 'prescribed fire', 'prescribed burning', 'water infiltration', 'soil hydraulic conductivity', 'surface runoff', 'soil loss'
95 and 'water erosion'. This bibliographic research returned 41 articles with 89 case studies.

96 In order to identify the key drivers of the changes in surface runoff and erosion rates in burned soils, the following
97 'environmental characteristics' were identified according to the relevant literature (Neary et al. 1999; Certini 2005;
98 Shakesby and Doerr 2006; Keeley 2009; Robichaud et al. 2010; Shakesby 2011; Moody et al. 2013; Alcañiz et al.
99 2018; Cole et al. 2020; Wagenbrenner et al. 2021; Agbeshie et al. 2022): (i) climate; (ii) soil slope; (iii) vegetation ;
100 (iv) soil burn severity; and (v) soil texture.

101 Of the 41 academic papers previously selected, only 21 (totalling 35 case studies) reported surface runoff and/or soil
102 erosion data in burned and unburned soils together with all the abovementioned environmental characteristics (Table
103 1).

104

105 *Data collection*

106

107 The 21 papers with the 35 case studies were carefully analysed, in order to compile a database in an Excel file. For
108 each case study, this database reported the values of the environmental characteristics as well as those of the
109 following quantitative variables: (i) rainfall depth (mm); (ii) water infiltration rate (mm/h); (iii) surface runoff
110 volume (mm); and (iv) soil loss (tons/ha). Rainfall intensity, which is a key variable for erosion predictions
111 (Wischmeier and Smith 1958; Liu et al. 2022), was excluded from the studied variables since the burned and
112 unburned sites were subjected to very similar precipitation (the difference being lower than 5%).

113

114 *Data processing*

115

116 The specific soil's hydrological response to prescribed fire was expressed quantitatively considering the four major
117 processes (precipitation, infiltration, runoff, soil erosion and transport) of soil hydrology (Moody et al. 2013). In
118 both unburned and burned state of each site, the hydrological and erosive variables (observations of water
119 infiltration, surface runoff, and soil loss) and environmental characteristics of the experimental sites were extracted
120 for the 35 case studies. In the case of burned sites this data was extracted at two dates: immediately after the
121 prescribed fire (hereafter 'short-term') and at the end of the monitoring period in the relevant study ('mid-term').
122 This separation in extraction dates was done to consider the different soil's hydrological response to fire throughout
123 the window of disturbance and the following period, when the pre-fire soil properties and vegetation cover are
124 progressively recovering.

125 The site in unburned condition was assumed to be the 'reference' or 'baseline' value for each of the four
126 investigated hydrological variables. For each case study, the so-called 'effect size' (e.g., Vieira et al. 2015; Girona-
127 García et al. 2021) for the change between the burned and the unburned sites was calculated for both the short and
128 mid-term. This effect size was estimated as the decimal logarithm (log) of the response ratio (Curtis and Wang
129 1998; Hedges et al. 1999) - hereafter 'log response ratio' (LRR) - using the following equation:

130

$$LRR = \log \frac{x_B}{x_{UB}} \quad (1)$$

131
132 where ' x_B ' is the mean value of the response variable measured in the site treated with prescribed fire (burned soil)
133 and ' x_{UB} ' is the corresponding value measured in the unburned condition at the same site. The value of the LRRs
134 expresses the magnitude of the impact of prescribed fire on a given soil on a logarithmic scale (e.g., Kalies et al.
135 2010). More specifically, a positive LRR means that the related hydrological variable in the burned site is higher,
136 and lower, if LRR is negative, as compared to the same variable at the unburned site. The exponent of LRR gives
137 the order of magnitude of the change. The four calculated LRRs are hereafter indicated as 'LRR(RF)' (for rainfall),
138 'LRR(WI)' (for water infiltration), 'LRR(SR)' (for surface runoff), and 'lnRR(SE)' (for soil erosion).
139 The wide range of site conditions and experimental observations, and the different methods adopted to measure the
140 studied variables do not impact the results of this analysis, since the calculation of the size effect was made in both
141 unburned and burned sites under the same conditions and monitoring period in each study (Vieira et al. 2015;
142 Girona-García et al. 2021).

143 The values of the environmental characteristics were grouped into classes to fix categorical variables, as follows:

- 144 (i) climate: continental; oceanic; temperate; semi-arid; tropical
- 145 (ii) soil slope (%): < 10; 10-20; 20-30; 30-40; 40-50; > 50
- 146 (iii) vegetation: grasses; shrubs; trees
- 147 (iv) soil burn severity: low; low to moderate; moderate; moderate to high; high
- 148 (v) soil texture: sandy; silty; clayey and combinations among these textural classes.

149
150 *Short description of prediction methods*

151
152 'Random Forests' or 'random decision forests' (hereafter 'RF') is a machine learning method used for the
153 classification and/or regression of variables of different types. For regression, RF predicts a quantitative dependent
154 variable based on: (i) independent quantitative and/or qualitative variables; (ii) continuous and discrete data.

155 The RF method creates a high number of so-called 'decision trees'. The latter is a structure,
156 where each internal node represents a test on an attribute, each branch represents the test result,
157 and each leaf represents a class label, that is a decision taken after computing all attributes. RF
158 consists of a combination of several decision trees that incorporate multiple bootstrap samples
159 from the observational data. Several input variables randomly participate in the construction of
160 each tree. Using the bootstrap method, many samples from the initial observations are
161 introduced. Then, a tree is expanded based on a bootstrap sample. Each tree produces a class
162 prediction and the class obtaining more votes than others becomes the model's prediction. Once
163 each whole tree is built, several trees are used as inputs to estimate the output variable. The
164 average value of these estimates gives the final output of the model (Avand et al. 2019). More
165 precisely, the outcome is a rank expressed in terms of mean decrease accuracy (or mean increase
166 error, which is the sum of the squares) as a prediction error. A larger value of this error means

167 that the importance of the related variable is higher for that model prediction (Mohammed et al.
168 2020).

169 A multiple-regression model (hereafter ‘MR’) builds a linear equation between a set of independent (‘predictor’ or
170 ‘explanatory’) variables on one side, and one dependent (or ‘response’) variable. The coefficients of the
171 independent variables are estimated by a regression method, for instance, the Minimum Least Square method. The
172 MR method develops a prediction equation under the following form:

$$LRR(SR) \text{ or } LRR(SE) = a + \sum_{i=1}^N b_i \cdot x_i \quad (2)$$

173 where:

- 174 - a = intercept
- 175 - b_i = model coefficients
- 176 - x_j = independent variables.

177
178 Partial Least Square Regression (hereafter ‘PLS-R’) is a regression method based on covariance, which is
179 recommended when the explanatory variables are numerous and multi-collinearity among the variables is possible.
180 PLS-R, having in general a non-linear structure, reduces the input variables to a smaller set of predictors
181 (‘component(s)’), which are used for regression.

182 A PLS-R method provides prediction equations under the following form:

$$LRR(SR) \text{ or } LRR(SE) = a + \sum_{i=1}^N b_i \cdot x_i + \sum_{j=1}^N \sum_{k=1}^N c_i \cdot x_j \cdot x_k \quad (3)$$

183 where:

- 184 - a = intercept
- 185 - b_i and c_i = model coefficients
- 186 - x_j and x_k = independent variables ($x_j \cdot x_k$ representing the non-linear term).

187

188 *Description of the case-studies*

189

190 In the thirty-five case studies in the selected 21 papers reporting data of surface runoff and soil erosion, 22 values of
191 runoff were related to the short-term observations (measured from immediately after the prescribed fire until 2-3
192 months later), and just as many to the mid-term observations (that is, at least one year after the prescribed fire). For
193 erosion, 17 observations were related to the short term, and 25 to the mid-term. Some papers reported both short-
194 term and mid-term observations, and many others both runoff and erosion values. All the categorical variables
195 related to the environmental characteristics for the 35 case studies are reported in Table 1.

196

Table 1 Main characteristics of the case studies used for modelling surface runoff and soil erosion by the three prediction methods

Case study	First author (year)	Journal	Country	Climate	Vegetation	Soil burn severity	Soil slope class (%)	Soil texture
1	González-Pelayo et al. (2010)	Geomorphology	Spain	Semi-arid	Shrubs	Low	21-30	Sandy loam
2	Cawson et al. (2013)	Forest Ecology and Management	Australia	Temperate	Trees	Low	41-50	Silty clay loam
3	Vega et al. (2005)	Land Degradation and Development	Spain	Oceanic	Shrubs	Low	21-30	Sandy loam
4			Spain	Oceanic	Shrubs	Low	21-30	Sandy loam
5	Morales et al. (2000)	Forest Ecology and Management	Mexico	Temperate	Trees	Low	11-20	Sand
6			Mexico	Temperate	Trees	Low	11-20	Sand
7	Townsend and Douglas (2000)	Journal of Hydrology	Australia	Tropical	Trees	Low	< 10	Sandy loam
8			Australia	Tropical	Trees	High	< 10	Sandy loam
9	Carrà et al. (2022)	Ecological Engineering	Italy	Semi-arid	Trees	Low	11-20	Loamy sand
10			Italy	Semi-arid	Trees	Low	11-20	Loamy sand
11			Italy	Semi-arid	Trees	Low	21-30	Loamy sand
12	Lucas-Borja et al. (2019)	Science of the Total Environment	Spain	Semi-arid	Trees	Low	11-20	Clay
13	Cawson et al. (2016)	Geoderma	Australia	Semi-arid	Trees	Low	41-50	Silty clay loam

14	Fernández et al. (2012)	Journal of Environmental Management	Spain	Semi-arid	Shrubs	Low	< 10	Sandy loam
15			Spain	Oceanic	Shrubs	Low	31-40	Sandy loam
16	Robichaud (2000)	Journal of Hydrology	USA	Continental	Trees	Low	41-50	Loam
17			USA	Continental	Trees	Low	> 50	Loam
18	Pierson et al. (2008)	Earth Surface Processes and Landforms	USA	Continental	Shrubs	Moderate to high	41-50	Sandy loam
19			USA	Continental	Shrubs	Moderate to high	41-50	Sandy loam
20	Zavala et al. (2009)	Earth Surface Processes and Landforms	Spain	Semi-arid	Shrubs	Low	< 10	Sandy loam + clayey loam
21	Pierson et al. (2014)	Rangeland Ecology Management	USA	Semi-arid	Trees	Low to moderate	11-20	Sandy loam
22			USA	Semi-arid	Trees	Low to moderate	11-20	Sandy loam
23			USA	Semi-arid	Trees	Low to moderate	11-20	Sandy loam
24			USA	Semi-arid	Trees	Low to moderate	11-20	Sandy loam
25	Carrà et al. (2021)	Hydrology	Italy	Semi-arid	Trees	Low	11-20	Loamy sand
26			Italy	Semi-arid	Trees	Low	11-20	Loamy sand

27			Italy	Semi-arid	Trees	Low	21-30	Loamy sand
28	Shakesby et al. (2015)	Catena	Portugal	Oceanic	Shrubs	Low to moderate	31-40	Loamy sand
29	Singh et al. (2017)	Forests	USA	Continental	Trees	Low	11-20	Silty loam
30			USA	Continental	Trees	Low	21-30	Silty loam
31			USA	Continental	Trees	Low	21-30	Silty loam
32			USA	Continental	Trees	Low	21-30	Silty loam
33	de Koff et al. (2006)	Soil Science	USA	Semi-arid	Shrubs	Low	> 50	Loam
34	Lucas-Borja et al. (2022)	Journal of Environmental Management	Spain	Semi-arid	Trees	Low	21-30	Sandy loam
35			Spain	Semi-arid	Trees	High	21-30	Sandy loam

200

201 For all prediction methods, two response variables were set, namely LRR(SR) and LRR(SE). In the first case, the
202 independent input parameters were the five categorical variables (climate, soil slope, soil burn severity, soil texture
203 and vegetation) as well as two quantitative variables, that is LRR(RF) and LRR(WI). In the second case, predicting
204 LRR(SE), the quantitative variable LRR(SR) was added to the set of independent categorical parameters.

205 The RF algorithm was applied using the ‘random input with replacement’ method with the ‘Mtry’ parameter set to
206 10 on the entire sample size (35 observations of surface runoff and just as many for soil erosion). The “bagging”
207 method was used as a sample bootstrap, in order to train each tree on the different subsets of observations. The
208 required number of trees in the forest was set to 100, which was equal to the number of trees built by the algorithm.

209 The MR analysis was applied selecting the most accurate set of independent variables as the best predictors. To
210 select the best model, the maximum r^2 was adopted as an objective function, and the Least Mean Square method was
211 used to calculate the model coefficients (a and b_i of equation 2).

212 PLS-R was applied to the case studies, adopting the ‘Jack-and-Knife’ cross-validation method. Table 3SI reports the
213 variable importance in equation 3, as provided by this method. The algorithm selects a set of derivative variables
214 (‘Components’) from the input parameters. We calculated the cumulated r^2_y and r^2_x , which measure the correlations
215 between the explanatory (x) and dependent (y) variables with these components. The variable significance in the
216 projections was also estimated, to identify the influence of each input parameter on the two response variables.

217 The three models were implemented using XLSTAT[®] software (release 2019).

218

219 *Evaluation of the model’s accuracy*

220

221 The prediction accuracy of the three models was analysed for ‘goodness-of-fit’ against the corresponding
222 observations adopting qualitative and quantitative approaches. The qualitative approach consisted of a visual
223 comparison of pairs of ‘observations’ vs. ‘predictions’ of LRR(SR) and LRR(SE) using scatterplots. For the
224 quantitative evaluation of model accuracy, we used the following indicators, commonly adopted in the literature
225 (e.g., Willmott 1982; Loague and Green 1991; Legates and McCabe Jr 1999): (a) the main statistics (maximum,
226 minimum, mean and standard deviation of observed and simulated values); (b) coefficient of determination (r^2); (c)
227 coefficient of efficiency of Nash and Sutcliffe (NSE, (Nash and Sutcliffe 1970)); (d) Root Mean Square Error
228 (RMSE); and (e) percentage bias (PBIAS). The studies by Van Liew and Garbrecht (2003), Krause et al. (2005) and
229 Moriasi et al. (2007) report the equations used to calculate the quantitative indicators mentioned above, while the
230 acceptance or optimal values are reported in Table 2. PBIAS, also known as the ‘coefficient of residual mass
231 (CRM)’ (Loague and Green 1991), is positive, when a model underestimates the observations, and negative in the
232 case of an overestimation (Gupta et al. 1999).

233

234 **Table 2** Indexes, their range of variability and acceptance/optimal values to evaluate the prediction capacity of the
 235 three prediction models
 236

Index	Range of variability	Acceptance limits or optimal values
r^2	0 to 1	$r^2 > 0.50$ (Santhi et al. 2001; Van Liew et al. 2003; Vieira et al. 2018b)
NSE	$-\infty$ to 1	Model accuracy: good, if $NSE \geq 0.75$; satisfactory, if $0.36 \leq NSE < 0.75$; unsatisfactory, if $NSE < 0.36$ (Van Liew et al. 2003)
RMSE	0 to ∞	$RMSE < 0.5$ of observed SD (Singh et al. 2005)
PBIAS	$-\infty$ to ∞	Model accuracy: fair, if PBIAS is 25% (for runoff) and $< 55\%$ (for erosion) (Moriasi et al. 2007)

237 Notes: r^2 = coefficient of determination; NSE = coefficient of efficiency of Nash and Sutcliffe; RMSE = Root Mean
 238 Square Error; PBIAS = percentage bias.

239

240

241 Results

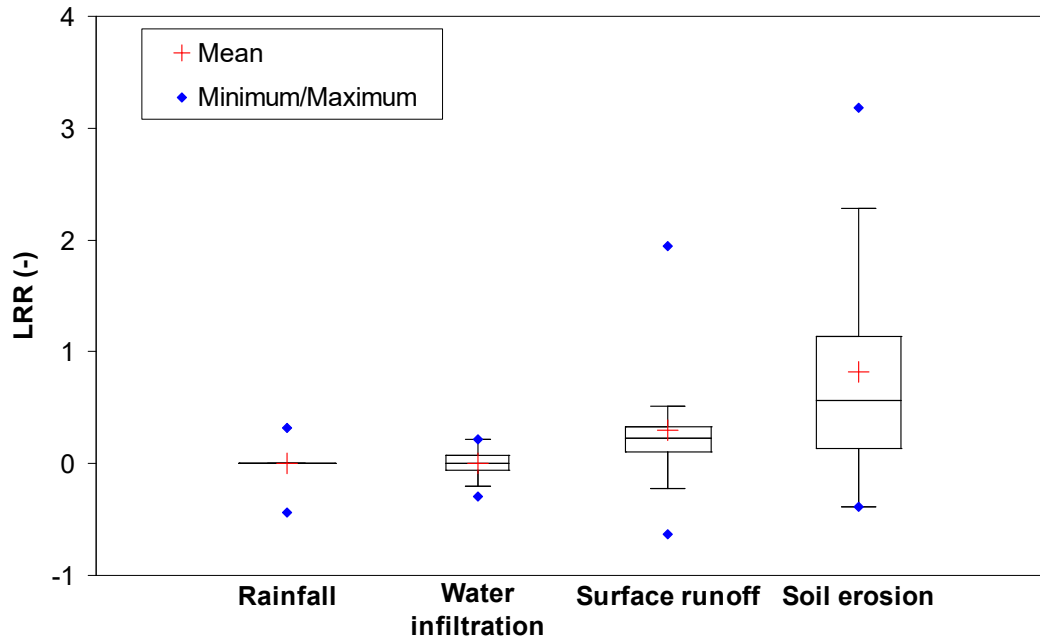
242

243 *Characterization of changes in rainfall, infiltration, runoff and erosion in the case studies*

244

245 LRR(RF) showed a very low variability in the selected case studies, from a minimum of -0.44 (case study 33, Table
 246 1) to a maximum of 0.32 (case studies 34 and 35). LRR(WI) was in the range of -0.30 (case study 18) to 0.22 (case
 247 study 20). In six cases (of which three were in the short term), infiltration was lower in burned sites compared to
 248 unburned sites (shown by negative LRRs), while, in the mid-term, water infiltration recovered the pre-fire levels,
 249 with three exceptions (case studies 24, 25 and 27) (Table 1 and Fig. 1).

250



251

252 **Fig. 1** Values of LRR (log response ratio) of rainfall, infiltration, runoff and erosion in the 35 case studies

253

254 The minimum LRR(SR) (-0.64) was found in case study 19, while case study 2 showed the maximum value (1.94).
 255 Surface runoff was always higher in burned sites compared to unburned sites in the short-term (positive LRRs),
 256 except in three case studies (13, 23 and 26). In the mid-term, surface runoff was generally lower in burned sites
 257 (case studies 18 to 20) (Fig. 1 and Table 1).

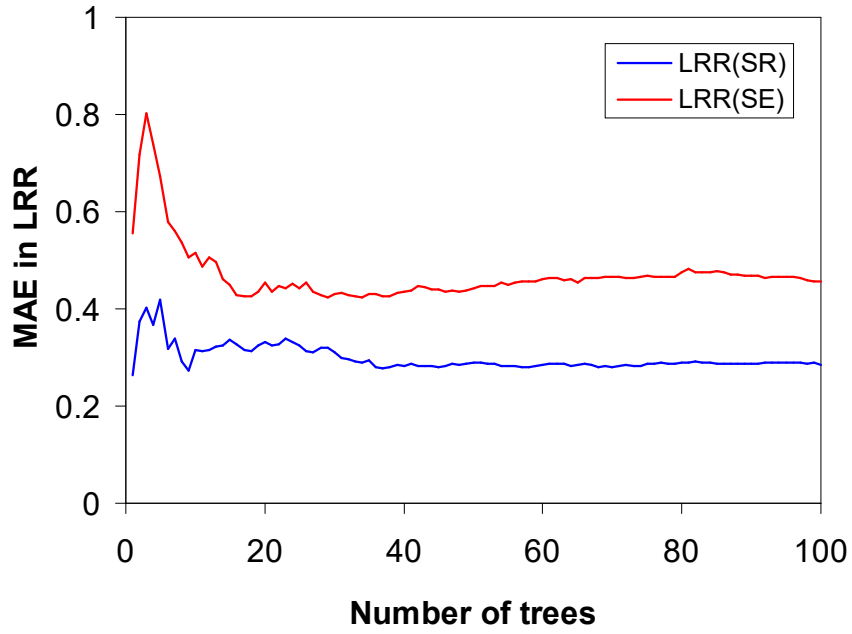
258 A similar pattern as that of the surface runoff was noticed in the short term for the changes in soil erosion. In more
 259 detail, LRR(SE) was always higher in burned sites compared to unburned sites (except for case study 23 in the short
 260 term and seven case studies in the mid-term). The lowest and highest values were found in the case studies 9 (-0.38)
 261 and 12 (3.19), respectively (Fig. 1 and Table 1).

262

263 *Model running*

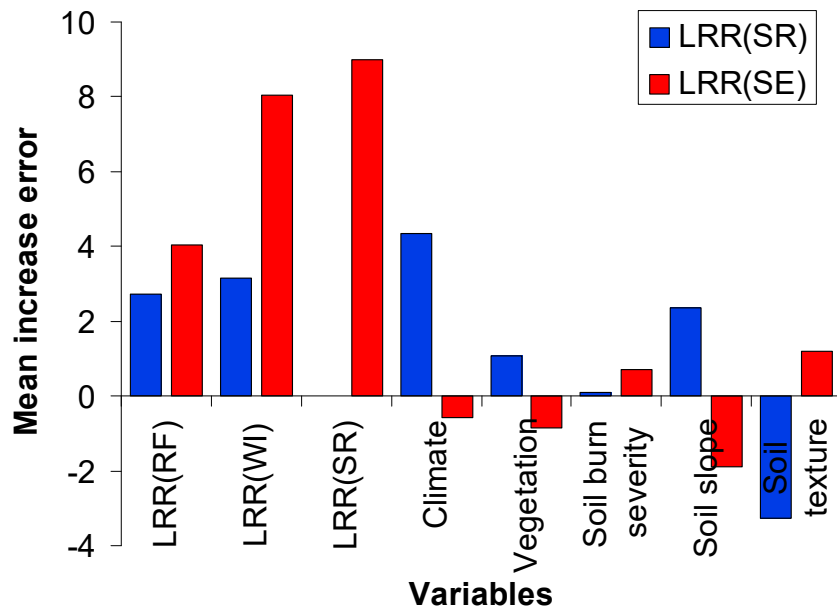
264

265 Of the 100 decision trees built by the RF model, 45 trees for LRR(SR) and 42 for LRR(SE) were needed to get the
 266 lowest and steady value of the minimum absolute error (MAE), which was on average 0.286 in the first case and
 267 0.462 in the second case (Fig. 2a).



268
269
270
271

(a)



272
273
274
275
276

(b)

Fig. 2 Variability of the Mean Absolute Error (MAE) with the number of trees (a) and mean increase error (b), expressing the importance of each input variable, in the Random Forest model applied to the case studies

277 For LRR(SR) predictions the most important input variables (identified using the highest mean increase errors) were
278 climate, LRR(RF), LRR(WI) and soil slope, while all the numerical variables (LRR of rainfall, infiltration and
279 runoff) were the most influential to predict LRR(SE) (Fig. 2b).
280 Regarding the MR analysis, a noticeable number of input variables were needed as best predictors of LRR(SR) and
281 LRR(SE). In more detail, the highest values of r^2 (0.516 for runoff and 0.674 for erosion) were achieved using 11
282 variables (climate, vegetation and soil texture groups) and 16 variables (LRR(RF), LRR(WI), LRR(SR), climate,
283 soil slope and soil texture), respectively (Table 3).

284 **Table 3** Variability of the coefficient of determination (r^2) with input variables in Equation (2) of the Multiple-Regression models applied to the case studies

285

Number of variables	Groups of variables	r^2
<i>LRR(SR)</i>		
10	Climate / Soil texture	0.250
11	Climate / Vegetation / Soil texture	0.516
12	LRR(WI) / Climate / Vegetation / Soil texture	0.507
13	LRR(RF) / LRR(WI) / Climate / Vegetation / Soil texture	0.491
14	LRR(RF) / LRR(WI) / Climate / Vegetation / Soil burn severity / Soil texture	0.474
18	LRR(RF) / LRR(WI) / Climate / Vegetation / Soil burn severity / Soil slope / Soil texture	0.451
<i>LRR(SE)</i>		
6	LRR(SR) / Soil slope	0.514
11	LRR(SR) / Climate / Soil texture	0.598
12	LRR(RF) / LRR(SR) / Climate / Soil texture	0.651
15	LRR(RF) / LRR(SR) / Climate / Soil slope / Soil texture	0.671
16	LRR(RF) / LRR(WI) / LRR(SR) / Climate / Soil slope / Soil texture	0.674
17	LRR(RF) / LRR(WI) / LRR(SR) / Climate / Vegetation / Soil slope / Soil texture	0.666
19	LRR(RF) / LRR(WI) / LRR(SR) / Climate / Vegetation / Soil burn severity / Soil slope / Soil texture	0.659

286 Note: the number in the first row indicates the total categorical or numeric variables of groups; the values in bold indicate the highest r^2 value with the selected input
 287 variables.

288

289 PLS-R selected only one derivative variable ('Component') from the selected dataset of input parameters. The
290 cumulated r^2_y and r^2_x between the independent and dependent variables with this component were low for LRR(SR)
291 (0.31 and 0.09, respectively), and higher (0.67 and 0.06) for LRR(SE).

292 The coefficients of the two regression (MR and PLS-R) models found respectively in equations 2 and 3 are reported
293 in Tables 1SI and 3SI, while Table 2SI shows the variable importance in predictions using the PLS-R model. It is
294 worth noting that only the PLS-R models used quantitative variables as input parameters, namely LRR(RF),
295 LRR(WI) and LRR(SR), while the MR analysis selected only categorical variables.

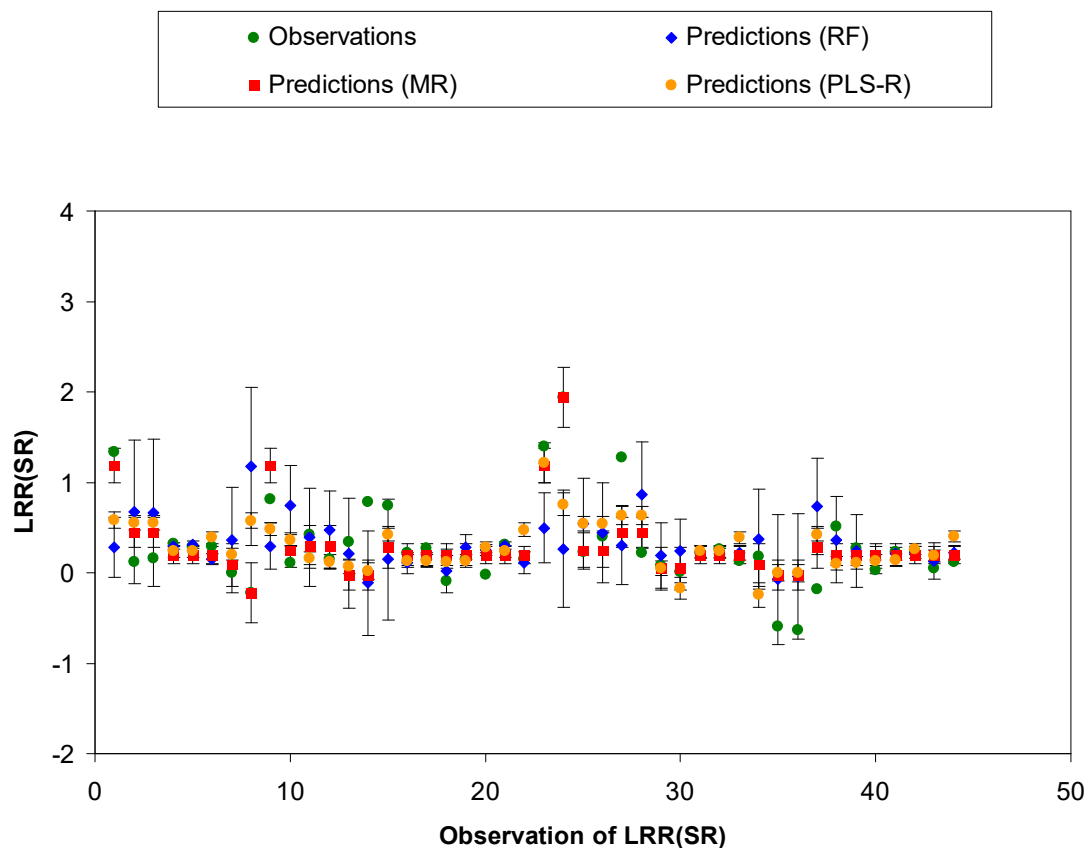
296

297 *Prediction accuracy of the three models*

298

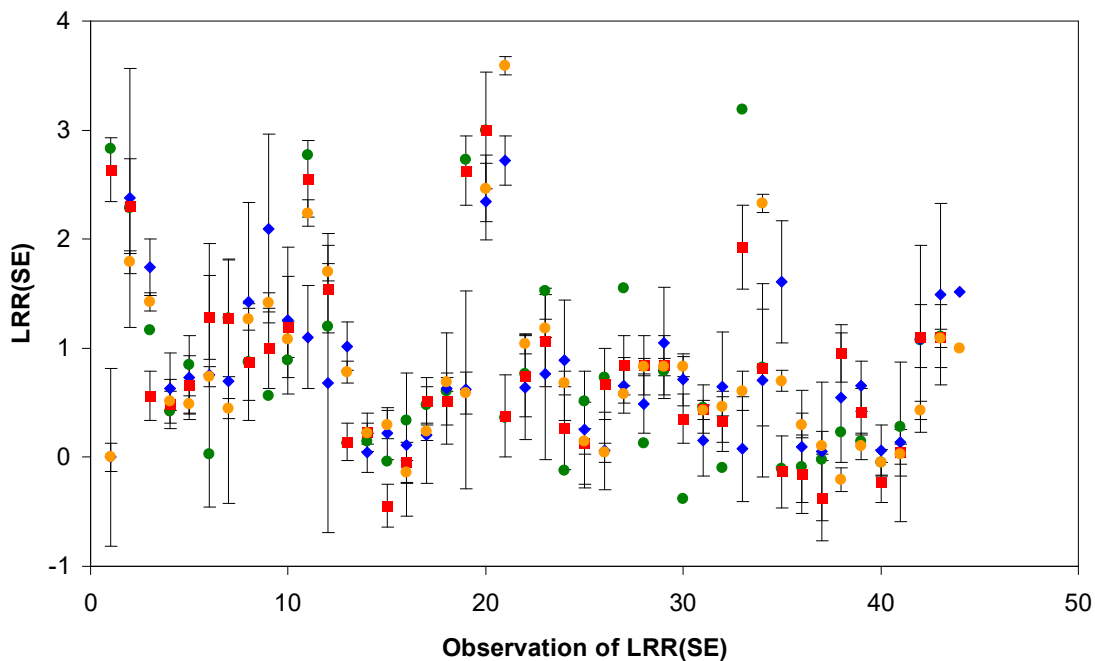
299 Figs. 3a and 3b depict the predictions of LRR(SR) and LRR(SE) using the three models in comparison to the
300 corresponding observations.

301



302

(a)



303

(b)

304 **Fig. 3** Prediction of LRR(SR) (a) and LRR(SE) (b) (mean \pm standard deviation) for each observation using three
305 models (RF = Random forest; MR = Multiple-Regression; PLS-R = Partial Least Square Regression) applied to the
306 case studies

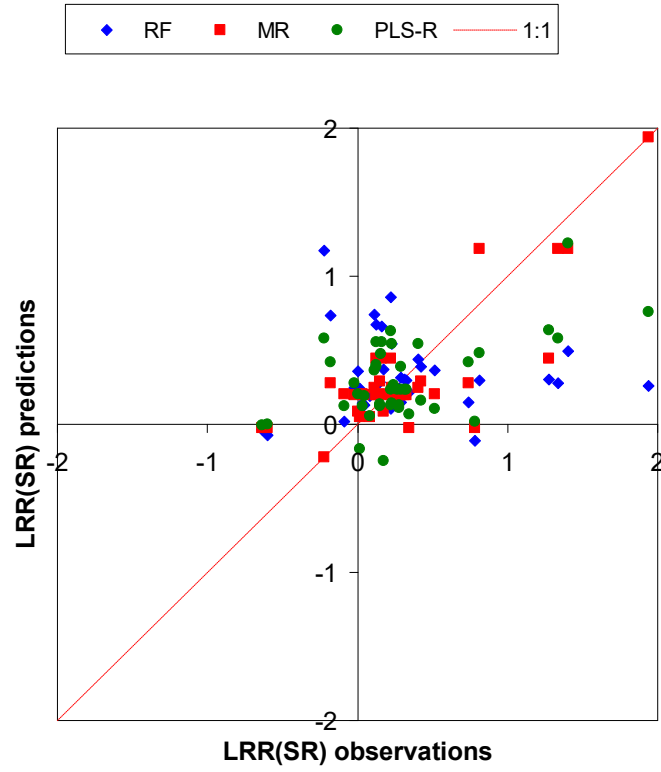
307

308

309 The RF algorithm gave poor predictions of changes in surface runoff. This is shown not only by the large scattering
310 of the 'observation vs. prediction' pairs along the line of perfect agreement (Fig. 4), but also by the poor values of
311 the evaluation indexes. In more detail, r^2 was zero, NSE was negative, and RMSE was higher compared to half the
312 observed standard deviation (Table 2). Therefore, all these indexes were far from the acceptable limits of Table 1.
313 RF accurately predicted the mean LRR(SR) (difference of 5.6% compared to the observed value), while the errors in
314 simulating the minimum and maximum LRRs were much higher (-82.3% and -39.5%). The algorithm showed a
315 very slight tendency to overestimate the observations of runoff changes (PBIAS of -0.06) (Table 4).

316 The predictions of LRR(SE) given by the RF algorithm were more reliable than the estimations LRR(SR) and, in
317 general, acceptable, although not good (r^2 and NSE equal to 0.47). There was no evidence of any model's tendency
318 towards overestimation or underestimation (PBIAS = -0.01) (Table 4). Overall, the model was more reliable in
319 simulating LRRs of erosion (differences of 1.3%, mean, and -14.6%, maximum) compared to the runoff predictions.

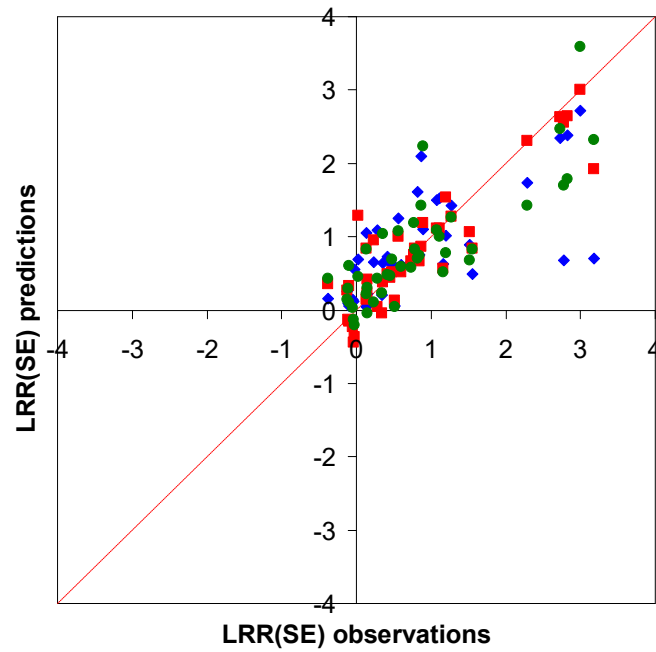
320



321

322

(a)



323

324

(b)

325 **Fig. 4** Scatterplot of observations vs. predictions of LRR(SR) (a) and LRR(SE) (b) using three models (RF =
326 Random forest; MR = Multiple-Regression; PLS-R = Partial Least Square Regression) applied to the case studies

327
328
329
330
331
332
333
334
335
336
337
338
339
340

The MR equations reproduced the observed LRRs with a different accuracy for runoff and erosion. In more detail, the scatterplot of LRR(SR) predicted by Eq. (2) shows a limited agreement between observations and predictions for intermediate values, while the lowest and highest LRRs fall close to the line of perfect agreement (Fig. 4). While RMSE got unsatisfactory values (0.28), r^2 and NSE values were satisfactory but not good (0.64 for both indexes). PBIAS was zero, thus indicating no under- or over-estimation of LRRs. However, the differences in the mean and maximum observed and predicted LRR(SR) were high (78.7% and 53.7%, respectively) (Table 4). In contrast, the Multiple-Regression Eq. (2) showed a very good capacity to predict the post-fire changes in erosion rates. The highest LRR(SE) was very close to the line of perfect agreement, and the same was noticed for most of the intermediate values (Fig. 4). Both r^2 and NSE were very high (0.80), PBIAS was zero (no under- or over-estimation), and RMSE was relatively low (-0.42, < 0.5 std. dev. of observations) (Table 4). Moreover, the mean and maximum LRR(SE) difference was zero or very low (-5.8%).

341 **Table 4** Indexes used to evaluate the LRR(SR) and LRR(SE) predictions using three models in the case studies

342

	LRR(SR)							
	<i>Mean</i>	<i>Minimum</i>	<i>Maximum</i>	<i>Standard deviation</i>	r^2	<i>E</i>	<i>PBIAS</i>	<i>RMSE</i>
	<i>Random Forest</i>							
Observation	0.297	-0.637	1.941	0.477	0.00	-0.29	-0.06	0.53
Prediction	0.314	-0.113	1.174	0.249				
	<i>Multiple-Regression</i>							
Observation	0.227	0.247	0.070	0.050	0.64	0.64	0.00	0.28
Prediction	0.405	0.247	0.108	0.050				
	<i>Partial Least Square Regression</i>							
Observation	0.297	-0.637	1.941	0.477	0.31	0.31	0.00	0.39
Prediction	0.297	-0.245	1.219	0.266				
	LRR(SE)							
	<i>Random Forest</i>							
Observation	0.821	-0.383	3.186	0.937	0.47	0.47	-0.01	0.68
Prediction	0.832	0.044	2.720	0.683				
	<i>Multiple-Regression</i>							
Observation	0.821	-0.383	3.186	0.937	0.80	0.80	0.00	0.42
Prediction	0.821	-0.446	3.000	0.838				
	<i>Partial Least Square Regression</i>							
Observation	0.821	-0.383	3.186	0.937	0.69	0.69	0.00	0.52
Prediction	0.821	-0.205	3.591	0.776				

343 Notes: r^2 : coefficient of determination; NSE: coefficient of efficiency of Nash and Sutcliffe; RMSE: Root Mean Square Error; PBIAS: coefficient of residual mass.

344

345 The simulations of runoff changes by PLS-R models were only acceptable, while a good prediction capacity was
346 noticed for LRR(SE). Regarding LRR(SR), r^2 and RMSE were poor (0.31 and 0.39, against a value of 0.48 of the
347 observed std. dev.) and NSE was positive but low (0.31). PBIAS was zero, indicating no under- or over-estimation of
348 LRRs, as also shown by the equal values of the observed and the predicted mean. In contrast, a noticeable
349 overestimation was observed for the minimum and maximum LRR values (-61.5% and -37.2%, respectively, Table 4),
350 as seen also in the related scatterplot (Fig. 4). The PLS-R model showed satisfactory predictions of LRR(SE), which is
351 shown by the appreciable values of r^2 (0.69), NSE (0.69), PBIAS (0) and RMSE (0.52, very close to half observed std.
352 dev.). However, while the predicted and observed values of mean and maximum LRR(SE) were equal or low, the
353 predictions of the minimum LRR data showed a difference of -46.6% compared to the corresponding observations
354 (Table 4).

355

356 **4. Discussion**

357

358 Prescribed fire noticeably alters the soil's hydrological and erosive response to the rainfall input (Cawson et al. 2012).
359 However, the post-fire runoff and erosion rates are site-specific, since it depends on the peculiar climatic, soil and
360 vegetal characteristics of the treated environment (Úbeda et al. 2018). This specificity is proved by the large variability
361 in water infiltration as well as in runoff and erosion already present in the selected case studies. In more detail, water
362 infiltration may decrease (as generally observed) but also increase (in a few case studies) after a prescribed fire. In the
363 papers analysed, post-fire infiltration was up to 50% lower in some sites (Pierson et al. 2008) in the short term, but case
364 studies with enhanced post-fire infiltration (up to +65%) are also reported (Zavala et al. 2009). The reduction in water
365 infiltration is mainly due to the changes in the most important physical properties of soil, such as the aggregate stability
366 (e.g., Fox et al. 2007; Arcenegui et al. 2008; Varela et al. 2010) and the occurrence of soil water repellency, which
367 induces hydrophobicity (Letey 2001; Cawson et al. 2016).

368 In the selected case studies, surface runoff and erosion rates generally showed a dramatic increase of up to 87-fold (for
369 runoff, Cawson et al. 2013) and 1500-fold (for erosion, Lucas-Borja et al. 2019) the values measured in the unburned
370 sites. Only in a few case studies, post-fire runoff and erosion were lower in the burned sites compared to the unburned
371 sites. The increase in the hydrological and erosive response of soil following the prescribed fire application is caused by
372 several factors (Cawson et al. 2012; Vieira et al. 2018a). In addition to the changes in infiltration rates and
373 hydrophobicity mentioned above, the almost total removal of vegetation and the noticeable modifications in some
374 important physicochemical properties of soil due to burning noticeably influence post-fire runoff and erosion (Certini
375 2005; Shakesby 2011; Moody et al. 2013; Alcañiz et al. 2018; Agbeshie et al. 2022). Moreover, since these impacts are
376 affected by high temporal variability, surface runoff and soil loss themselves are variable over time (Prosser and
377 Williams 1998). In this regard, the selected case studies showed a general recovery of the pre-fire values some years
378 after the fire, although in some case studies the mid-term runoff and erosion rates remained noticeably high, despite
379 being a long time since the fire application.

380 The variability in soil hydrology after a prescribed fire, and the unsteady character of the soil's hydrological response
381 over time make the simulation of post-fire surface runoff and erosion processes particularly challenging (Vieira et al.
382 2015; Lopes et al. 2021; Girona-García et al. 2021). This difficulty explains the contrasting prediction accuracy shown
383 by the three models evaluated in the selected case studies, with the RF algorithm showing a low prediction accuracy,
384 and regression models performing much better.

385 In more detail, one of the main advantages of RF algorithms is reproducibility and high transparency of feature
386 importance (Wilder et al. 2021). However, the predictions of changes in runoff and erosion by the algorithms
387 developed in this study were poor in reproducing the first case and acceptable (but not optimal) for the second variable.
388 The poor RF performance in modelling post-fire runoff led to large overestimations of the measured variable. This
389 inaccuracy may be explained by two reasons. First, the algorithm may have found severe problems in modelling such a
390 high number of categorical variables (presumably the addition of a third quantitative variable smoothed this model's
391 inaccuracy for erosion simulations). Second, the training dataset was limited. In contrast algorithms of artificial
392 intelligence (AI) generally require many observations (Singh et al. 2016). Regarding previous applications of RF
393 algorithms tools to predict surface runoff and erosion (Wilder et al. 2021) showed that two RF models better predicted
394 the impacts of post-fire peak streamflow in small semi-arid watersheds compared to empiric methods, and these
395 algorithms helped to identify critical watershed characteristics driving the flooding risk. Moreover, Ghosh and Maiti
396 (2021) assessed the probability of severe erosion in sub-tropical watersheds using RF tools, showing its higher
397 prediction accuracy compared to a logistic regression model. Furthermore, the results of the study by Mohammed et al.
398 (2020) carried out in Mediterranean semi-arid hillslopes affected by severe erosion showed the higher prediction
399 accuracy of RF algorithms compared to general linear models. RF models also performed better than other machine
400 learning techniques in predicting soil erosion in tropical plots (Tarek et al. 2023) and k-Nearest Neighbor Classifiers in
401 mapping gully erosion susceptibility in arid and semi-arid catchments (Avand et al. 2019). Past experiences of AI tools
402 used to model post-fire soil hydrology were scarce. Only Folharini et al. (2022) used RF and Support Vector Machine
403 algorithms for hydrological simulations in small burned catchments of Northern Portugal, and found a satisfactory
404 prediction accuracy in modelling soil erosion (r^2 between 0.54 and 0.68). In a pine forest in Central-Eastern Spain,
405 Zema et al. (2020) tested an Artificial Neural Network, which gave good predictions for both runoff and soil erosion
406 (NSE > 0.90).

407 In this study, the prediction capacity of the MR and PLS-R models provided mixed results. In the case of runoff
408 predictions, the two models were not able to reproduce the mean and maximum values. This is a poor result since the
409 models are not able to estimate, as a minimum, the order of magnitude of changes in the runoff rates due to prescribed
410 fire application in a specific environment. Moreover, both models were inaccurate in trying to simulate every log
411 response ratio of runoff, and this limits the model transferability from one environment to another. These results
412 contrast with those achieved by Lucas-Borja et al. (2020), who reported a NSE of 0.60 (in sites burned by prescribed
413 fires) and 0.73 (in unburned soils) using MR linear equations to predict surface runoff in Mediterranean semi-arid
414 forests. In contrast, the PLS-R performed reasonably well and the MR equation was very accurate in modelling the
415 changes in post-fire erosion. The better prediction capacity shown by the two models for erosion simulations may be
416 due to the addition of a third quantitative variable to the log response ratios of rainfall and infiltration used for runoff
417 modelling. The worse performance of the PLS-R model compared to the MR equation could be explained by the loss of
418 variance due to the need for the addition of non-linear terms in equation (3), which may have propagated measurement
419 errors in the model. In contrast, the MR model retained several categorical variables (without any errors). In the latter
420 model, it is worth mentioning the importance of some key variables that drive the runoff and soil loss generation
421 mechanisms, such as the climate type and soil texture (for runoff and erosion) as well as the soil slope (for erosion). The
422 patterns of precipitation that turn to surface runoff change with site climate (e.g., Molinié et al. 2012; Li et al. 2022) and
423 soil texture (e.g., Cawson et al. 2012; Alcañiz et al. 2018). Climate governs rainfall erosivity (and thus an important
424 share of erosion), which is higher in dry climates and lower in oceanic and continental areas (e.g., Capolongo et al.
425 2008; Nearing et al. 2017) Soil slope is influential on the processes of soil detachment and transport (e.g., Wischmeier

426 and Smith (1978) and Lucas-Borja et al. 2020). However, in this analysis we must highlight the lack of measurements
427 in many of the studies reviewed, which did not report a key variable for runoff and generation mechanisms in burned
428 soils, such as the post-fire ground cover. Surface runoff and soil loss may result in very different rates between bare
429 soils and sites covered by plants. Vegetation intercepts rainwater, increases evapo-transpiration, reduces rainsplash
430 erosion, and slowdowns both overland and concentrated water flows (e.g., Shakesby and Doerr 2006; Zhang et al.
431 2023). This promotes the idea that this variable is essential for accurate predictions of both runoff and erosion. In other
432 words, the accuracy of the evaluated models may increase, if the post-fire ground cover is considered as an input
433 variable by the algorithms or regression equations. The good prediction capacity of erosion that was found for the MR
434 model developed in this study agrees with the results of the study by Zema et al. (2022). These authors estimated runoff
435 coefficients and sediment concentrations (from which soil loss can be estimated) using two multiple-regression models
436 that adopted a limited set of input parameters related to ground cover (e.g., litter, shrub vegetation, ash, bare soil
437 percentage) and ‘dummy’ categorical variables. The quantitative evaluation of the prediction capacity of the models
438 gave NSE over 0.85 for runoff coefficients and 0.95 for soil losses, which are close to the values of the same index
439 calculated in this study.

440

441 **5. Conclusions**

442

443 This study has evaluated three models (a Random Forest algorithm and two Multiple-Regression and Partial Least
444 Square Regression equations) applied to case studies selected from the international scientific literature, to predict the
445 changes in surface runoff and soil erosion in sites treated with prescribed fire under different environmental
446 characteristics.

447 The Random Forest showed a poor performance in simulating runoff, but an acceptable capacity to predict soil loss.
448 The prediction capacity to simulate runoff shown by the Multiple-Regression and Partial Least Square Regression
449 equations was satisfactory but not optimal, while the performance in simulating erosion was good using the Multiple-
450 Regression equation.

451 The Random Forest model proposed in this study is a novelty in its application to areas treated with prescribed fire, and
452 the potentiality of this machine learning tool for hydrological predictions deserves more research. The limited number
453 of case studies of the modelling exercise in this study may have influenced the RF’s poor performance.

454 The good performance of the Multiple-Regression model in simulating erosion in soils treated with prescribed fire is
455 encouraging. Although the applicability of Multiple-Regression models in burned environments has been tested
456 previously, their adaptation to the case studies in this study has shown how the parameters of their equations may be
457 used for modelling purposes in areas with similar climatic and geomorphological characteristics as the experimental
458 sites.

459 Overall, considering the scarce applications of hydrological and/or erosive models in natural sites treated with
460 prescribed fire that have been carried out on a global scale, this study helps land managers and hydrologists to select the
461 most accurate prediction model to be adopted to control and mitigate the wildfire and hydrogeological risks in delicate
462 environments, such as forest ecosystems.

463

464 **References**

465

466 Agbeshie AA, Abugre S, Atta-Darkwa T, Awuah R (2022) A review of the effects of forest fire on
467 soil properties. *Journal of Forestry Research* 1–23

468 Aksoy H, Kavvas ML (2005) A review of hillslope and watershed scale erosion and sediment
469 transport models. *Catena* 64:247–271

470 Alcañiz M, Outeiro L, Francos M, Úbeda X (2018) Effects of prescribed fires on soil properties: A
471 review. *Science of the Total Environment* 613:944–957

472 Arcenegui V, Mataix-Solera J, Guerrero C, et al (2008) Immediate effects of wildfires on water
473 repellency and aggregate stability in Mediterranean calcareous soils. *Catena* 74:219–226

474 Avand, Janizadeh, Naghibi, et al (2019) A Comparative Assessment of Random Forest and k-
475 Nearest Neighbor Classifiers for Gully Erosion Susceptibility Mapping. *Water* 11:2076.
476 <https://doi.org/10.3390/w11102076>

477 Beyene MT, Leibowitz SG, Dunn CJ, Bladon KD (2023) To burn or not to burn: An empirical
478 assessment of the impacts of wildfires and prescribed fires on trace element concentrations in
479 Western US streams. *Science of The Total Environment* 863:160731.
480 <https://doi.org/10.1016/j.scitotenv.2022.160731>

481 Cao X, Hu X, Han M, et al (2022) Characteristics and predictive models of hillslope erosion in
482 burned areas in Xichang, China, on March 30, 2020. *CATENA* 217:106509.
483 <https://doi.org/10.1016/j.catena.2022.106509>

484 Capolongo D, Diodato N, Mannaerts Cm, et al (2008) Analyzing temporal changes in climate
485 erosivity using a simplified rainfall erosivity model in Basilicata (southern Italy). *Journal of*
486 *Hydrology* 356:119–130

487 Carrà BG, Bombino G, Denisi P, et al (2021) Water Infiltration after Prescribed Fire and Soil
488 Mulching with Fern in Mediterranean Forests. *Hydrology* 8:95

489 Carrà BG, Bombino G, Lucas-Borja ME, et al (2022) Prescribed fire and soil mulching with fern in
490 Mediterranean forests: Effects on surface runoff and erosion. *Ecological Engineering* 176:106537

491 Carra BG, Bombino G, Lucas-Borja ME, et al (2021) Modelling the Event-Based Hydrological
492 Response of Mediterranean Forests to Prescribed Fire and Soil Mulching with Fern Using the Curve
493 Number, Horton and USLE-Family (Universal Soil Loss Equation) Models. *Land* 10:1166

494 Cawson JG, Nyman P, Smith HG, et al (2016) How soil temperatures during prescribed burning
495 affect soil water repellency, infiltration and erosion. *Geoderma* 278:12–22.
496 <https://doi.org/10.1016/j.geoderma.2016.05.002>

497 Cawson JG, Sheridan GJ, Smith HG, Lane PNJ (2012) Surface runoff and erosion after prescribed
498 burning and the effect of different fire regimes in forests and shrublands: a review. *International*
499 *Journal of Wildland Fire* 21:857–872

500 Cawson JG, Sheridan GJ, Smith HG, Lane PNJ (2013) Effects of fire severity and burn patchiness
501 on hillslope-scale surface runoff, erosion and hydrologic connectivity in a prescribed burn. *Forest
502 Ecology and Management* 310:219–233. <https://doi.org/10.1016/j.foreco.2013.08.016>

503 Certini G (2005) Effects of fire on properties of forest soils: a review. *Oecologia* 143:1–10

504 Coelho C de OA, Ferreira AJD, Boulet A-K, Keizer JJ (2004) Overland flow generation processes,
505 erosion yields and solute loss following different intensity fires. *Quarterly Journal of Engineering
506 Geology and Hydrogeology* 37:233–240

507 Cole RP, Bladon KD, Wagenbrenner JW, Coe DBR (2020) Hillslope sediment production after
508 wildfire and post - fire forest management in northern California. *Hydrological Processes* 34:5242–
509 5259. <https://doi.org/10.1002/hyp.13932>

510 Curtis PS, Wang X (1998) A meta-analysis of elevated CO₂ effects on woody plant mass, form, and
511 physiology. *Oecologia* 113:299–313. <https://doi.org/10.1007/s004420050381>

512 de Dios Benavides-Solorio J, MacDonald LH (2005) Measurement and prediction of post-fire
513 erosion at the hillslope scale, Colorado Front Range. *International Journal of Wildland Fire* 14:457–
514 474

515 de Koff JP, Graham RC, Hubbert KR, Wohlgemuth PM (2006) Prefire and postfire erosion of soil
516 nutrients within a chaparral watershed: *Soil Science* 171:915–928.
517 <https://doi.org/10.1097/01.ss.0000235231.02063.c2>

518 Fernández C, Vega JA (2016) Evaluation of RUSLE and PESERA models for predicting soil
519 erosion losses in the first year after wildfire in NW Spain. *Geoderma* 273:64–72.
520 <https://doi.org/10.1016/j.geoderma.2016.03.016>

521 Fernández C, Vega JA (2018) Evaluation of the rusle and disturbed wepp erosion models for
522 predicting soil loss in the first year after wildfire in NW Spain. *Environmental Research* 165:279–
523 285. <https://doi.org/10.1016/j.envres.2018.04.008>

524 Fernández C, Vega JA, Fonturbel T (2012) The effects of fuel reduction treatments on runoff,
525 infiltration and erosion in two shrubland areas in the north of Spain. *Journal of Environmental
526 Management* 105:96–102. <https://doi.org/10.1016/j.jenvman.2012.03.048>

527 Folharini S, Vieira A, Bento-Gonçalves A, et al (2022) Soil Erosion Quantification using Machine
528 Learning in Sub-Watersheds of Northern Portugal. *Hydrology* 10:7.
529 <https://doi.org/10.3390/hydrology10010007>

530 Fox DM, Darboux F, Carrega P (2007) Effects of fire - induced water repellency on soil aggregate
531 stability, splash erosion, and saturated hydraulic conductivity for different size fractions.
532 *Hydrological Processes: An International Journal* 21:2377–2384

533 Ghosh A, Maiti R (2021) Soil erosion susceptibility assessment using logistic regression, decision
534 tree and random forest: study on the Mayurakshi river basin of Eastern India. *Environmental Earth*
535 *Sciences* 80:1–16

536 Girona-García A, Vieira DCS, Silva J, et al (2021) Effectiveness of post-fire soil erosion mitigation
537 treatments: A systematic review and meta-analysis. *Earth-Science Reviews* 217:103611.
538 <https://doi.org/10.1016/j.earscirev.2021.103611>

539 González-Pelayo O, Andreu V, Gimeno-García E, et al (2010) Rainfall influence on plot-scale
540 runoff and soil loss from repeated burning in a Mediterranean-shrub ecosystem, Valencia, Spain.
541 *Geomorphology* 118:444–452

542 Gupta HV, Sorooshian S, Yapo PO (1999) Status of automatic calibration for hydrologic models:
543 Comparison with multilevel expert calibration. *Journal of hydrologic engineering* 4:135–143

544 Hedges LV, Gurevitch J, Curtis PS (1999) The meta-analysis of response ratios in experimental
545 ecology. *Ecology* 80:1150–1156. [https://doi.org/10.1890/0012-](https://doi.org/10.1890/0012-9658(1999)080[1150:TMAORR]2.0.CO;2)
546 [9658\(1999\)080\[1150:TMAORR\]2.0.CO;2](https://doi.org/10.1890/0012-9658(1999)080[1150:TMAORR]2.0.CO;2)

547 Hosseini M, Nunes JP, Pelayo OG, et al (2018) Developing generalized parameters for post-fire
548 erosion risk assessment using the revised Morgan-Morgan-Finney model: A test for north-central
549 Portuguese pine stands. *CATENA* 165:358–368. <https://doi.org/10.1016/j.catena.2018.02.019>

550 Hueso-González P, Martínez-Murillo JF, Ruiz-Sinoga JD (2018) Prescribed fire impacts on soil
551 properties, overland flow and sediment transport in a Mediterranean forest: A 5 year study. *Science*
552 *of The Total Environment* 636:1480–1489. <https://doi.org/10.1016/j.scitotenv.2018.05.004>

553 Kalies EL, Chambers CL, Covington WW (2010) Wildlife responses to thinning and burning
554 treatments in southwestern conifer forests: a meta-analysis. *Forest Ecology and Management*
555 259:333–342

556 Karamesouti M, Petropoulos GP, Papanikolaou ID, et al (2016) Erosion rate predictions from
557 PESERA and RUSLE at a Mediterranean site before and after a wildfire: Comparison &
558 implications. *Geoderma* 261:44–58. <https://doi.org/10.1016/j.geoderma.2015.06.025>

559 Keeley JE (2009) Fire intensity, fire severity and burn severity: a brief review and suggested usage.
560 *International journal of wildland fire* 18:116–126

561 Keesstra SD, Maroulis J, Argaman E, et al (2014) Effects of controlled fire on hydrology and
562 erosion under simulated rainfall. *Cuadernos de Investigación Geográfica* 40:269–294

563 Klimas K, Hiesl P, Hagan D, Park D (2020) Prescribed fire effects on sediment and nutrient exports
564 in forested environments: A review. *J environ qual* 49:793–811. <https://doi.org/10.1002/jeq2.20108>

565 Krause P, Boyle DP, Bäse F (2005) Comparison of different efficiency criteria for hydrological
566 model assessment. *Advances in geosciences* 5:89–97

567 Larsen IJ, MacDonald LH (2007) Predicting postfire sediment yields at the hillslope scale: Testing
568 RUSLE and Disturbed WEPP: PREDICTING POSTFIRE SEDIMENT YIELDS. *Water Resour*
569 *Res* 43:. <https://doi.org/10.1029/2006WR005560>

570 Legates DR, McCabe Jr GJ (1999) Evaluating the use of “goodness - of - fit” measures in
571 hydrologic and hydroclimatic model validation. *Water resources research* 35:233–241

572 Letey J (2001) Causes and consequences of fire - induced soil water repellency. *Hydrological*
573 *Processes* 15:2867–2875

574 Li J, Sun R, Chen L (2022) Assessing the accuracy of large-scale rainfall erosivity estimation based
575 on climate zones and rainfall patterns. *Catena* 217:106508

576 Liu J, Liang Y, Gao G, et al (2022) Quantifying the effects of rainfall intensity fluctuation on runoff
577 and soil loss: From indicators to models. *Journal of Hydrology* 607:127494

578 Loague K, Green RE (1991) Statistical and graphical methods for evaluating solute transport
579 models: overview and application. *Journal of contaminant hydrology* 7:51–73

580 Lopes AR, Girona - García A, Corticeiro S, et al (2021) What is wrong with post - fire soil erosion
581 modelling? A meta - analysis on current approaches, research gaps, and future directions. *Earth*
582 *Surf Process Landforms* 46:205–219. <https://doi.org/10.1002/esp.5020>

583 Lucas-Borja ME, Bombino G, Carrà BG, et al (2020) Modeling the Soil Response to Rainstorms
584 after Wildfire and Prescribed Fire in Mediterranean Forests. *Climate* 8:150.
585 <https://doi.org/10.3390/cli8120150>

586 Lucas-Borja ME, de las Heras J, Moya Navarro D, et al (2022) Short-term effects of prescribed
587 fires with different severity on rainsplash erosion and physico-chemical properties of surface soil in
588 Mediterranean forests. *Journal of Environmental Management* 322:116143.
589 <https://doi.org/10.1016/j.jenvman.2022.116143>

590 Lucas-Borja ME, Plaza-Álvarez PA, Gonzalez-Romero J, et al (2019) Short-term effects of
591 prescribed burning in Mediterranean pine plantations on surface runoff, soil erosion and water
592 quality of runoff. *Science of The Total Environment* 674:615–622

593 Merritt WS, Letcher RA, Jakeman AJ (2003) A review of erosion and sediment transport models.
594 *Environmental modelling & software* 18:761–799

595 Mohammed S, Al-Ebraheem A, Holb IJ, et al (2020) Soil management effects on soil water erosion
596 and runoff in central Syria—A comparative evaluation of general linear model and random forest
597 regression. *Water* 12:2529

598 Molinié G, Ceresetti D, Anquetin S, et al (2012) Rainfall regime of a mountainous Mediterranean
599 region: Statistical analysis at short time steps. *Journal of Applied Meteorology and Climatology*
600 51:429–448

601 Moody JA, Shakesby RA, Robichaud PR, et al (2013) Current research issues related to post-
602 wildfire runoff and erosion processes. *Earth-Science Reviews* 122:10–37

603 Morales HA, Návar J, Domínguez PA (2000) The effect of prescribed burning on surface runoff in
604 a pine forest stand of Chihuahua, Mexico. *Forest Ecology and Management* 137:199–207.
605 [https://doi.org/10.1016/S0378-1127\(99\)00328-X](https://doi.org/10.1016/S0378-1127(99)00328-X)

606 Moriasi DN, Arnold JG, Van Liew MW, et al (2007) Model evaluation guidelines for systematic
607 quantification of accuracy in watershed simulations. *Transactions of the ASABE* 50:885–900

608 Morris RH, Bradstock RA, Dragovich D, et al (2014) Environmental assessment of erosion
609 following prescribed burning in the Mount Lofty Ranges, Australia. *Int J Wildland Fire* 23:104.
610 <https://doi.org/10.1071/WF13011>

611 Nash JE, Sutcliffe JV (1970) River flow forecasting through conceptual models part I—A
612 discussion of principles. *Journal of hydrology* 10:282–290

613 Nearing MA, Yin S, Borrelli P, Polyakov VO (2017) Rainfall erosivity: An historical review.
614 *Catena* 157:357–362

615 Neary DG, Klopatek CC, DeBano LF, Ffolliott PF (1999) Fire effects on belowground
616 sustainability: a review and synthesis. *Forest ecology and management* 122:51–71

617 Pierson FB, Robichaud PR, Moffet CA, et al (2008) Soil water repellency and infiltration in coarse-
618 textured soils of burned and unburned sagebrush ecosystems. *CATENA* 74:98–108.
619 <https://doi.org/10.1016/j.catena.2008.03.011>

620 Pierson FB, Williams CJ, Kormos PR, Al-Hamdan OZ (2014) Short-Term Effects of Tree Removal
621 on Infiltration, Runoff, and Erosion in Woodland-Encroached Sagebrush Steppe. *Rangeland
622 Ecology & Management* 67:522–538. <https://doi.org/10.2111/REM-D-13-00033.1>

623 Prosser IP, Williams L (1998) The effect of wildfire on runoff and erosion in native Eucalyptus
624 forest. *Hydrological processes* 12:251–265

625 Robichaud PR (2000) Fire effects on infiltration rates after prescribed fire in Northern Rocky
626 Mountain forests, USA. *Journal of Hydrology* 231–232:220–229. [https://doi.org/10.1016/S0022-
627 1694\(00\)00196-7](https://doi.org/10.1016/S0022-1694(00)00196-7)

628 Robichaud PR, Ashmun LE, Sims BD (2010) Post-fire treatment effectiveness for hillslope
629 stabilization. U.S. Department of Agriculture, Forest Service, Rocky Mountain Research Station,
630 Ft. Collins, CO

631 Rulli MC, Offeddu L, Santini M (2013) Modeling post-fire water erosion mitigation strategies.
632 *Hydrology and Earth System Sciences* 17:2323–2337. <https://doi.org/10.5194/hess-17-2323-2013>

633 Salis M, Giudice LD, Robichaud PR, et al (2019) Coupling wildfire spread and erosion models to
634 quantify post-fire erosion before and after fuel treatments. *Int J Wildland Fire* 28:687–703.
635 <https://doi.org/10.1071/WF19034>

636 Santhi C, Arnold JG, Williams JR, et al (2001) Validation of the swat model on a large river basin
637 with point and nonpoint sources 1. *JAWRA Journal of the American Water Resources Association*
638 37:1169–1188

639 Shakesby RA (2011) Post-wildfire soil erosion in the Mediterranean: review and future research
640 directions. *Earth-Science Reviews* 105:71–100

641 Shakesby RA, Bento CPM, Ferreira CSS, et al (2015) Impacts of prescribed fire on soil loss and
642 soil quality: An assessment based on an experimentally-burned catchment in central Portugal.
643 *CATENA* 128:278–293. <https://doi.org/10.1016/j.catena.2013.03.012>

644 Shakesby RA, Doerr SH (2006) Wildfire as a hydrological and geomorphological agent. *Earth-*
645 *Science Reviews* 74:269–307

646 Singh A, Thakur N, Sharma A (2016) A review of supervised machine learning algorithms. In:
647 2016 3rd International Conference on Computing for Sustainable Global Development
648 (INDIACom). Ieee, pp 1310–1315

649 Singh G, Schoonover J, Monroe K, et al (2017) Prescribed Burning and Erosion Potential in Mixed
650 Hardwood Forests of Southern Illinois. *Forests* 8:112. <https://doi.org/10.3390/f8040112>

651 Singh J, Knapp HV, Arnold JG, Demissie M (2005) Hydrological modeling of the Iroquois river
652 watershed using HSPF and SWAT 1. *JAWRA Journal of the American Water Resources*
653 *Association* 41:343–360

654 Soulis KX (2018) Estimation of SCS Curve Number variation following forest fires. *Hydrological*
655 *Sciences Journal* 63:1332–1346. <https://doi.org/10.1080/02626667.2018.1501482>

656 Tarek Z, Elshewey AM, Shohieb SM, et al (2023) Soil Erosion Status Prediction Using a Novel
657 Random Forest Model Optimized by Random Search Method. *Sustainability* 15:7114.
658 <https://doi.org/10.3390/su15097114>

659 Townsend SA, Douglas MM (2000) The effect of three fire regimes on stream water quality, water
660 yield and export coefficients in a tropical savanna (northern Australia). *Journal of Hydrology*
661 229:118–137. [https://doi.org/10.1016/S0022-1694\(00\)00165-7](https://doi.org/10.1016/S0022-1694(00)00165-7)

662 Úbeda X, Pereira P, Badía D (2018) Prescribed fires. *Science of The Total Environment* 637–
663 638:385–388. <https://doi.org/10.1016/j.scitotenv.2018.04.272>

664 Van Liew MW, Arnold JG, Garbrecht JD (2003) Hydrologic simulation on agricultural watersheds:
665 Choosing between two models. *Transactions of the ASAE* 46:1539

666 Van Liew MW, Garbrecht J (2003) Hydrologic simulation of the little Washita river experimental
667 watershed using SWAT 1. *JAWRA Journal of the American Water Resources Association* 39:413–
668 426

669 Varela ME, Benito E, Keizer JJ (2010) Effects of wildfire and laboratory heating on soil aggregate
670 stability of pine forests in Galicia: The role of lithology, soil organic matter content and water
671 repellency. *Catena* 83:127–134

672 Vega JA, Fernández C, Fonturbel T (2005) Throughfall, runoff and soil erosion after prescribed
673 burning in gorse shrubland in Galicia (NW Spain): THROUGHFALL, RUNOFF AND EROSION
674 AFTER BURNING. *Land Degrad Dev* 16:37–51. <https://doi.org/10.1002/ldr.643>

675 Vieira DCS, Fernández C, Vega JA, Keizer JJ (2015) Does soil burn severity affect the post-fire
676 runoff and interrill erosion response? A review based on meta-analysis of field rainfall simulation
677 data. *Journal of Hydrology* 523:452–464. <https://doi.org/10.1016/j.jhydrol.2015.01.071>

678 Vieira DCS, Malvar MC, Martins MAS, et al (2018a) Key factors controlling the post-fire
679 hydrological and erosive response at micro-plot scale in a recently burned Mediterranean forest.
680 *Geomorphology* 319:161–173

681 Vieira DCS, Serpa D, Nunes JPC, et al (2018b) Predicting the effectiveness of different mulching
682 techniques in reducing post-fire runoff and erosion at plot scale with the RUSLE, MMF and
683 PESERA models. *Environmental Research* 165:365–378.
684 <https://doi.org/10.1016/j.envres.2018.04.029>

685 Wagenbrenner JW, Ebel BA, Bladon KD, Kinoshita AM (2021) Post-wildfire hydrologic recovery
686 in Mediterranean climates: A systematic review and case study to identify current knowledge and
687 opportunities. *Journal of Hydrology* 126772

688 Wilder BA, Lancaster JT, Cafferata PH, et al (2021) An analytical solution for rapidly predicting
689 post - fire peak streamflow for small watersheds in southern California. *Hydrological Processes*
690 35:. <https://doi.org/10.1002/hyp.13976>

691 Willmott CJ (1982) Some comments on the evaluation of model performance. *Bulletin of the*
692 *American Meteorological Society* 63:1309–1313

693 Wischmeier WH, Smith DD (1958) Rainfall energy and its relationship to soil loss. *Eos,*
694 *Transactions American Geophysical Union* 39:285–291

695 Wischmeier WH, Smith DD (1978) Predicting rainfall erosion losses: a guide to conservation
696 planning. Department of Agriculture, Science and Education Administration

697 Zavala LM, Jordán A, Gil J, et al (2009) Intact ash and charred litter reduces susceptibility to rain
698 splash erosion post-wildfire. *Earth Surf Process Landforms* 34:1522–1532.
699 <https://doi.org/10.1002/esp.1837>

700 Zema DA, Carrà BG, Lucas-Borja ME (2022) Exploring and Modeling the Short-Term Influence of
701 Soil Properties and Covers on Hydrology of Mediterranean Forests after Prescribed Fire and
702 Mulching. *Hydrology* 9:21. <https://doi.org/10.3390/hydrology9020021>
703 Zema DA, Lucas-Borja ME, Fotia L, et al (2020) Predicting the hydrological response of a forest
704 after wildfire and soil treatments using an Artificial Neural Network. *Computers and Electronics in*
705 *Agriculture* 170:105280
706 Zhang Y, Yuan C, Chen N, Levia DF (2023) Rainfall partitioning by vegetation in China: A
707 quantitative synthesis. *Journal of Hydrology* 617:128946.
708 <https://doi.org/10.1016/j.jhydrol.2022.128946>
709

710 **Supplementary Information**

711

712 **Table 1SI** Values of the coefficients a and b in equation 2 of the Multiple-Regression model used to predict LRR(SR)
713 and LRR(SE) in the case studies

714

Variables (x_i and x_j in equation 1)	Model coefficients	
	LRR(SR)	LRR(SE)
Intercept (a in equation 1)	-0.374	1.591
LRR(RF)	0	1.862
LRR(WI)	0	1.686
LRR(SR)	0	2.064
Climate(Continental)	-1.058	-0.819
Climate(Oceanic)	-0.784	-0.600
Climate(Semiarid)	0.153	-0.632
Climate(Temperate)	2.315	-3.373
Climate(Tropical)	0	0
Vegetation (Shrubs)	0.983	0
Vegetation(Trees)	0	0
Soil burn severity(Low)	0	0
Soil burn severity(Low to moderate)	0	0
Soil burn severity(Moderate to high)	0	0
Soil burn severity(High)	0	0
Soil slope(< 10%)	0	-1.110
Soil slope(11%-20%)	0	-0.783
Soil slope(21%-30%)	0	-0.608
Soil slope(31%-40%)	0	0.392
Soil slope(41%-50%)	0	0.731
Soil slope(> 50%)	0	0
Soil texture(Sand)	-1.495	0
Soil texture(Loam)	1.721	0
Soil texture(Clay)	0.309	1.065
Soil texture(Loamy sand)	0.419	-0.325
Soil texture(Sandy loam)	0.422	-0.517
Soil texture(Silty loam)	0	0

Soil texture(Silty clay loam)	0	0
Soil texture(Sandy loam + clayey loam)	-0.482	-0.213

715

716

Table 2SI Values of the coefficients a , b and c in equation 3 of the Partial Least Square Regression model used to predict LRR(SR) and LRR(SE) in the case studies

Variables (x_i and x_j in equation 1)	Model coefficients	
	LRR(SR)	LRR(SE)
Intercept (a in equation 1)	0.287	0.822
LRR(RF)	-0.036	0.025
LRR(WI)	-0.012	-0.030
LRR(SR)	0	0.164
Climate(Continental)	-0.103	0.003
Climate(Oceanic)	-0.022	0.081
Climate(Semiarid)	-0.011	-0.062
Climate(Temperate)	0.205	0.574
Climate(Tropical)	-0.106	-0.168
Vegetation(Shrubs)	0.055	0.133
Vegetation(Trees)	-0.055	-0.133
Soil burn severity(Low)	0.104	0.082
Soil burn severity(Low to moderate)	-0.048	-0.108
Soil burn severity(Moderate to high)	-0.145	0.012
Soil burn severity(High)	-0.117	-0.022
Soil slope(< 10%)	-0.002	-0.097
Soil slope(11%-20%)	-0.048	-0.146
Soil slope(21%-30%)	0.105	0.071
Soil slope(31%-40%)	-0.078	0.176
Soil slope(41%-50%)	-0.003	0.140
Soil slope(> 50%)	-0.060	0.001
Soil texture(Sand)	0.067	0.000
Soil texture(Loam)	-0.004	0.001
Soil texture(Clay)	-0.089	0.212
Soil texture(Loamy sand)	-0.056	-0.014
Soil texture(Sandy loam)	-0.002	-0.080

Soil texture(Silty loam)	-0.006	-0.006
Soil texture(Silty clay loam)	0.240	0.355
Soil texture(Sandy loam + clayey loam)	-0.007	-0.064
LRR(RF) • LRR(WI)	0.067	0
LRR(RF) • LRR(WI)	0.492	0
LRR(RF) • LRR(SR)	-0.457	0
LRR(RF) • Climate(Continental)	-0.058	0
LRR(RF) • Climate(Oceanic)	0.027	0
LRR(RF) • Climate(Semiarid)	0.030	0
LRR(RF) • Climate(Temperate)	-9.602	0
LRR(RF) • Climate(Tropical)	-0.504	0
LRR(RF) • Vegetation(Shrubs)	0.001	0
LRR(RF) • Vegetation(Trees)	0.077	0
LRR(RF) • Soil burn severity(Low)	0.021	0
LRR(RF) • Soil burn severity(Low to moderate)	0.032	0
LRR(RF) • Soil burn severity(Moderate to high)	-0.202	0
LRR(RF) • Soil burn severity(High)	0.026	0
LRR(RF) • Soil slope (< 10%)	-0.441	0
LRR(RF) • Soil slope(11%-20%)	0.605	0
LRR(RF) • Soil slope(21%-30%)	0.002	0
LRR(RF) • Soil slope(31%-40%)	0.026	0
LRR(RF) • Soil slope(41%-50%)	-2.307	0
LRR(RF) • Soil slope(> 50%)	0	0
LRR(RF) • Soil texture(Loam)	0	0
LRR(RF) • Soil texture(Clay)	0.553	0
LRR(RF) • Soil texture(Loamy sand)	0.028	0
LRR(RF) • Soil texture(Sandy loam)	-0.001	0
LRR(RF) • Soil texture(Silty loam)	0.099	0
LRR(RF) • Soil texture-Sandy loam + clayey loam	1.055	0
LRR(RF) • Soil texture(Silty clay loam)	-5.898	0

LRR(WI) • LRR(SR)	0.046	0
LRR(WI) • Climate(Continental)	-0.040	0
LRR(WI) • Climate(Oceanic)	0.063	0
LRR(WI) • Climate(Semiarid)	-0.026	0
LRR(WI) • Climate(Temperate)	0.000	0
LRR(WI) • Climate(Tropical)	0.000	0
LRR(WI) • Vegetation(Shrubs)	-0.029	0
LRR(WI) • Vegetation(Trees)	-0.036	0
LRR(WI) • Soil burn severity(Low)	-0.016	0
LRR(WI) • Soil burn severity(Low to moderate)	-0.036	0
LRR(WI) • Soil burn severity(Moderate to high)	-0.040	0
LRR(WI) • Soil burn severity(High)	0.000	0
LRR(WI) • Soil slope (< 10%)	-0.022	0
LRR(WI) • Soil slope(11%-20%)	-0.036	0
LRR(WI) • Soil slope(21%-30%)	0.000	0
LRR(WI) • Soil slope(31%-40%)	0.063	0
LRR(WI) • Soil slope(41%-50%)	-0.040	0
LRR(WI) • Soil slope(> 50%)	0.000	0
LRR(WI) • Soil texture(Clay)	0.000	0
LRR(WI) • Soil texture(Loam)	0.000	0
LRR(WI) • Soil texture(Loamy sand)	0.000	0
LRR(WI) • Soil texture(Sandy loam)	-0.033	0
LRR(WI) • Soil texture(Silty loam)	0.000	0
LRR(WI) • Soil texture(Silty clay loam)	0.000	0
LRR(WI) • Soil texture(Sandy loam + clayey loam)	-0.025	0
LRR(SR) • Climate(Continental)	0.161	0
LRR(SR) • Climate(Oceanic)	0.177	0
LRR(SR) • Climate(Semiarid)	0.170	0

Table 3SI Variable importance in predictions using equation 3 of the Partial Least Square Regression model used to predict LRR(SR) and LRR(SE) in the case studies

Variable	LRR(SR)	Variable	LRR(SE)
LRR(RF) • Vegetation(Shrubs)	2.392	LRR(SR)	3.740
Climate(Temperate)	2.271	LRR(RF) • LRR(SR)	2.697
Soil texture(Silty clay loam)	1.739	LRR(SR) • Climate(Semiarid)	2.566
Soil burn severity(Low)	1.657	LRR(RF) • Soil slope(11%-20%)	2.479
Soil burn severity(Moderate to high)	1.451	LRR(RF) • Soil texture(Clay)	2.204
Soil slope(21%-30%)	1.407	Climate(Temperate)	2.000
LRR(RF) • Climate(Semiarid)	1.274	LRR(RF) • Climate(Temperate)	2.000
LRR(RF)	1.235	LRR(RF) • Climate(Continental)	1.736
Climate(Continental)	1.231	Soil texture(Silty clay loam)	1.731
LRR(RF) • Climate(Continental)	1.231	LRR(RF) • Soil texture(Silty clay loam)	1.725
Soil texture(Loamy sand)	0.865	Soil slope(11%-20%)	1.609
Vegetation (Shrubs)	0.853	Vegetation(Shrubs)	1.469
Vegetation(Trees)	0.853	Vegetation(Trees)	1.469
Soil slope(11%-20%)	0.834	Soil slope(41%-50%)	1.121
Climate(Tropical)	0.769	LRR(RF) • Soil slope(41%-50%)	1.114
LRR(RF) • Climate(Tropical)	0.769	Soil burn severity(Low to moderate)	1.054
LRR(RF) • Climate(Temperate)	0.755	Soil slope(31%-40%)	1.037
Soil texture(Sand)	0.667	Soil texture(Clay)	1.030

Soil texture(Clay)	0.646	LRR(RF) • Vegetation(Trees)	0.996
Soil burn severity(Low to moderate)	0.643	Soil burn severity(Low)	0.929
Soil burn severity(High)	0.610	Soil texture(Sandy loam)	0.918
LRR(WI)	0.429	Climate(Tropical)	0.819
LRR(RF) • LRR(WI)	0.429	LRR(RF) • Climate(Tropical)	0.819
Soil slope(31%-40%)	0.404	LRR(WI) • LRR(SR)	0.779
Soil slope(> 50%)	0.314	Soil slope(21%-30%)	0.751
LRR(RF) • Vegetation(Trees)	0.210	LRR(RF) • Soil slope (< 10%)	0.742
Climate(Oceanic)	0.191	Soil slope(< 10%)	0.721
LRR(RF) • Climate(Oceanic)	0.191	Climate(Semiarid)	0.690
Climate(Semiarid)	0.187	LRR(WI) • LRR(SR)	0.679
Soil texture(Sandy loam + clayey loam)	0.053	LRR(WI)	0.679
Soil slope(41%-50%)	0.037	LRR(WI) • Climate(Continental)	0.635
Soil texture(Sandy loam)	0.035	LRR(WI) • Soil burn severity(Moderate)	0.635
Soil texture(Loam)	0.025	LRR(WI) • Soil slope(41%-50%)	0.635
Soil slope(< 10%)	0.017	LRR(WI) • Soil texture(Silty clay loam)	0.622
		LRR(WI) • Vegetation(Shrubs)	0.618
		Climate(Oceanic)	0.601
		LRR(RF)	0.582
		LRR(RF) • Climate(Semiarid)	0.558
		LRR(RF) • Soil burn severity(Low to moderate)	0.423
		LRR(WI) • Climate(Semiarid)	0.406

	LRR(RF) • Soil texture(Loamy sand)	0.382
	LRR(RF) • Climate(Oceanic)	0.356
	LRR(RF) • Soil slope(31%-40%)	0.349
	LRR(RF) • Soil burn severity(Low)	0.347
	LRR(SR) • Climate(Oceanic)	0.324
	Soil texture(Sandy loam + clayey loam)	0.310
	LRR(RF) • Soil texture(Sandy loam + clayey loam)	0.310
	LRR(WI) • Soil texture(Sandy loam + clayey loam)	0.310
	LRR(WI) • Soil slope (< 10%)	0.301
	LRR(WI) • Vegetation(Trees)	0.286
	LRR(WI) • Soil burn severity(Low to moderate)	0.286
	LRR(WI) • Soil slope(11%-20%)	0.286
	LRR(WI) • Climate(Oceanic)	0.238
	LRR(WI) • Soil slope(31%-40%)	0.238
	LRR(WI) • Soil burn severity(High)	0.231
	LRR(WI) • Soil burn severity(Low)	0.225
	Soil burn severity(High)	0.129
	Soil texture(Loamy sand)	0.126
	LRR(RF) • Soil burn severity(Moderate to high)	0.082
	Soil burn severity(Moderate to high)	0.082
	Soil texture(Silty loam)	0.040
	LRR(RF) • Soil texture(Silty loam)	0.040

	LRR(WI) • Climate(Continental)	0.031
	Climate(Continental)	0.031
	LRR(RF) • Soil slope(21%-30%)	0.023
	LRR(RF) • Vegetation(Shrubs)	0.019
	LRR(RF) • Soil texture(Sandy loam)	0.013
	Soil slope(> 50%)	0.003
	Soil texture(Loam)	0.003
	LRR(RF) • Soil slope(> 50%)	0.003
	LRR(RF) • Soil texture(Loam)	0.003
	LRR(WI) • Climate(Temperate)	0
	LRR(WI) • Climate(Tropical)	0
	LRR(WI) • Soil burn severity(High)	0
	LRR(WI) • Soil slope(21%-30%)	0
	LRR(WI) • Soil slope(> 50%)	0
	LRR(WI) • Soil texture(Clay)	0
	LRR(WI) • Soil texture(Loam)	0
	LRR(WI) • Soil texture(Loamy sand)	0
	LRR(WI) • Soil texture(Silty clay loam)	0
	LRR(WI) • Soil texture(Silty loam)	

Note: the values in bold indicate the highest values (over a limit of 0.80).